# Aqueous Organometallic Chemistry of Ruthenium(II). Aquo Carbonyl Derivatives and Related Ethene Hydrocarboxylation in Fully Aqueous Solvent

**Tiziana Funaioli,*,† Claudia Cavazza,† Fabio Marchetti,‡ and Giuseppe Fachinetti*,†**

Dipartimento di Chimica e Chimica Industriale, Università di Pisa, via Risorgimento 35, I-56126 Pisa, Italy, and Dipartimento di Ingegneria Chimica, dei Materiali delle Materie Prime e Metallurgia, Università Degli Studi di Roma "La Sapienza", via del Castro Laurenziano, 7, I-00195 Roma, Italy

*Received December 14, 1998*

A series of new water soluble and stable organometallic compounds is reported, and the peculiar role of water in their formation and stabilization is documented together with their catalytic properties in aqueous solution. The complex *fac*-$Ru(OCOCF_3)_2(CO)_3(H_2O)$ (**1**) constitutes the entry to a new type of aqueous organometallic chemistry. The substitution of trifluoroacetato ligands by $H_2O$ yields $[fac\text{-}Ru(CO)_3(H_2O)_3]^{2+}$ (**2**), isolated as the tetrafluoroborate derivative, the first structurally characterized complex bearing CO and $H_2O$ ligands only. In water, **2** undergoes nucleophilic attack by the solvent yielding $[fac\text{-}Ru(COOH)(CO)_2(H_2O)_3]^{+}$ (**3**), followed by $CO_2$ elimination to give $[fac\text{-}RuH(CO)_2(H_2O)_3]^{+}$ (**4**), a ruthenium(II) hydride devoid of group-15-donor coligands and stable toward strong acids. **4** inserts ethene in water to give $[fac\text{-}Ru(C_2H_5)(CO)_2(H_2O)_3]^{+}$ (**5**), an exceptionally inert alkyl complex which inserts CO yielding $[fac\text{-}Ru(C(O)C_2H_5)(CO)_2(H_2O)_3]^{+}$ (**6**). Attempts to isolate the mononuclear cationic acyl complex gave the tetranuclear $Ru_4(C(O)C_2H_5)_4(OH)_2(CF_3SO_3)_2(CO)_8$ (**7**). At 140 °C the mononuclear organometallic complexes become labile intermediates of a Reppe hydrocarboxylation of ethene in fully aqueous solvent.

## Introduction

In industrial organic chemistry water is regarded as an advantageous solvent: it is cheap and environmentally compatible and allows a low-cost recovery of the water-soluble catalyst in those catalytic processes resulting in a water/substrate−product two-phase system.[1] A class of water-soluble catalytic precursors employs ligands with peripheral hydrophilic functions;[2] for instance, the Rh(I) complex with sulfonated triphenylphosphane is the water-soluble catalyst in the recently developed Ruhrchemie/Rhône-Poulenc hydroformylation process of propene to butyraldehyde.[3] In this case water is merely a convenient reaction medium, while the catalytic reaction is similar to that in an organic solvent. On the other hand, water-soluble catalysts can be obtained by employing water itself as a ligand. In these cases, water is a critical ligand on the active catalytic species: due to its intrinsic properties (ionizing power, H-bonding ability, strongly coordinating power), peculiar features are then expected for both the catalytic process and related organometallic chemistry. However, only a few examples of catalytic processes promoted by aquo complexes in water are known[4] and elementary processes in organometallic chemistry are still to be documented in water as solvent. We report here the direct observation in water of the fundamental organometallic reactions as required for ethene activation. The water-soluble hydrido−, alkyl−, and acyl−aquo carbonyl complexes thus encountered become, at high temperature, intermediates of the catalytic hydrocarboxylation of ethene[5] in fully aqueous solvent.

## Experimental Section

**General Methods.** Unless otherwise specified, all manipulations were performed in air and in $H_2O$. AR grade acetone, diglyme, diethyl ether, diethyl acetate, toluene, $D_2O$, $CF_3COOH$, $CF_3SO_3H$, and $HBF_4$ as the diethyl ether adduct were purchased from Aldrich and used without further purification. CO and ethene were purchased from Matheson, and $^{13}CO$ (99% isotopical purity) was purchased from Aldrich. Ruthenium trichloride hydrate was used as received from Chimet SpA. The ruthenium complexes $Ru_3(CO)_{12}$[6] and *fac*-$Ru(OCOCF_3)_2(CO)_3[(CH_3)_2CHOH]$[7] were prepared by literature methods. The IR spectra were recorded with a Perkin-Elmer Model FT-IR 1725-X spectrophotometer and the $^1H$ and $^{13}C$ NMR spectra with a Varian Model Gemini-200 spectrometer. Liquid samples for infrared spectra were recorded in a 0.1 mm thick $CaF_2$ cell. $CO_2$ was determined by purging the solutions and reaction vessels with argon, bubbling the gases through aliquots of a 0.110 N $Ba(OH)_2$ solution, and back-titrating (phenolphthalein end point) the excess of $Ba(OH)_2$. Organic products were analyzed with a Dani Model 8400 gas chromatograph equipped with a flame ionization detector and a 2 m Carbowax packed column, previously washed with acid; ethane/ethene mixtures were analyzed with a 2 m Carboxen-1004 micropacked column. The apparatus and

† Università di Pisa.
‡ Università Degli Studi di Roma "La Sapienza".

(1) Horváth, I. T.; Joó, F. *Aqueous Organometallic Chemisty and Catalysis*; Kluwer Academic Publishers: Dordrecht, **1995**.
(2) (a) Hermann, W. A.; Kohlpainter, C. W. *Angew. Chem., Int. Ed. Engl.* **1993**, *32*, 1524. (b) Darensbourg, D. J.; Decuir, T. J.; Stafford, N. W.; Robertson, J. B.; Draper, J. D.; Reibenspies, J. H.; Kathò, A.; Joò, F. *Inorg. Chem.* **1997**, *36*, 4218 and references therein.
(3) Kuntz, E. G. *CHEMTECH* **1987**, 570.
(4) (a) Laurenczy, G.; Merbach, A. E. *J. Chem. Soc., Chem. Commun.* **1993**, 187. (b) McGrath, D. V.; Grubbs, R. H. *Organometallics* **1994**, *13*, 224. (c) Novak, B. M.; Grubbs, R. H. *J. Am. Chem. Soc.* **1988**, *110*, 7542.
(5) Reppe, J. W.; Reindl, E. *Justus Leibigs Ann. Chem.* **1953**, *582*, 121.
(6) Braca, G.; Sbrana, G.; Pino, P. *Chim. Ind. (Milan)* **1964**, *46*, 206; **1968**, *50*, 121.
(7) Fachinetti, G.; Funaioli, T.; Lecci, L.; Marchetti, F. *Inorg. Chem.* **1996**, *35*, 7217.

10.1021/ic981429i CCC: $18.00 
Published on Web 06/17/1999

procedures for the gas-volumetric measurements have been described.[8] Catalytic runs were carried out in a 400 mL rocking stainless steel autoclave charged with 50 mL aliquots of an aqueous 0.01 M solution of [*fac*-$Ru(C(O)C_2H_5)(CO)_2(H_2O)_3][CF_3SO_3]$ containing variable amounts of triflic acid and pressurized with ethene (30 atm) under a variable $P_{CO}$. The autoclave was immersed in an oil bath at 140 °C.

***fac*-$Ru(OCOCF_3)_2(CO)_3(H_2O)$ (1).** *fac*-$Ru(OCOCF_3)_2(CO)_3[(CH_3)_2CHOH]$[7] (7.0 g, 14.86 mmol) was dissolved in 100 mL of water-saturated $Et_2O$ and the solution evaporated to dryness (60 °C, 0.1 mmHg); this operation was repeated once more. Colorless crystals of **1** (5.77 g, 13.45 mmol, 90.5% yield) were obtained from acetone/diethyl acetate. IR of the solid product as Nujol mull: $\nu_{CO}$ 2153 s, 2094 vs, and 2079 vs $cm^{-1}$. IR in 0.5 M $CF_3COOH$: $\nu_{CO}$ 2152 s, 2088 vs $cm^{-1}$. The molecular structure of **1** is shown in Figure 1. A $^{13}CO$-enriched sample of **1** was obtained by performing the disproportionation step[7] of the synthesis of *fac*-$Ru(OCOCF_3)_2(CO)_3[(CH_3)_2CHOH]$ under a $^{13}CO$ atmosphere.

**[*fac*-$Ru(CO)_3(H_2O)_3]^{2+}$ (2). (a) Tetrafluoroborate.** $HBF_4 \cdot Et_2O$ (2.8 mL, 19.4 mmol) was added to **1** (2.37 g, 5.52 mmol) dissolved in 140 mL of $Et_2O$ saturated with $H_2O$. The solution was evaporated to dryness (60 °C, 0.1 mmHg), leaving a sticky residue, which became solid when washed with anhydrous $Et_2O$ (2.15 g, 5.2 mmol, 94.3% yield). The solid deliquesces in air at high relative humidity and gives large colorless crystals back in dry air. The molecular structure is shown in Figure 3. IR of the solid product as Nujol mull: $\nu_{CO}$ 2181 s, 2122 vs $cm^{-1}$. IR in 0.5 M $HBF_4$: $\nu_{CO}$ 2160 s, 2095 vs $cm^{-1}$. IR of a freshly prepared 0.04 M $D_2O$ solution shows absorptions of an equilibrium mixture of **2** ($\nu_{CO}$: 2160 w, 2095 m $cm^{-1}$) and **3** [*fac*-$Ru(COOD)(CO)_2(H_2O)_3]^+$ (2075 s, 2004 s, 1616 m $cm^{-1}$); on addition of $HBF_4$ 0.5 M, the 2160 s and 2095 vs $cm^{-1}$ absorptions were immediately restored. $^{13}C$ NMR of $^{13}C$-enriched [*fac*-$Ru(CO)_3(H_2O)_3][BF_4]_2$ in $D_2O$/0.5 M $HBF_4$: 183.0 ppm. $^{13}C$ NMR of a freshly prepared $D_2O$ solution: 183.0, 184.4, 185.5, 186.1, 194.1, 194.8, and 196.9 ppm. On addition of 0.5 M $HBF_4$, only the 183 ppm resonance became observable.

**(b) Triflate. 1** (24 g, 55.94 mmol) was suspended in 100 mL of $H_2O$ containing 11 mL (124.7 mmol) of triflic acid and evaporated to dryness (150 °C, 0.01 mmHg). On cooling, the viscous pale brown residue solidified and a vitreous material analyzing as $Ru(CF_3SO_3)_2(CO)_3(H_2O)$ was obtained in a substantially quantitative yield. An aqueous solution of this material displays the same IR and NMR spectra as reported above for the tetrafluoroborate derivative.

**[*fac*-$RuH(CO)_2(H_2O)_3]^+$ (4). 2** (50 mL of a 0.04 M solution) as the di-tetrafluoroborato or di-triflato derivative was allowed to stand at room temperature under an argon atmosphere. Within 3 h, the IR absorptions of **2** ($\nu_{CO}$: 2160 w, 2095 m $cm^{-1}$) and [*fac*-$Ru(COOH)(CO)_2(H_2O)_3]^+$ (**3**) (2075 s, 2004 s $cm^{-1}$) in equilibrium were replaced by absorptions at 2343 and 2053 s, 1973 s $cm^{-1}$. Evolution of $CO_2$ in a 1:1 molar ratio to ruthenium was determined. An aliquot of the solution was potentiometrically titrated with 0.1 M NaOH. The solution (5.0 mL) was reduced under vacuum to 1.0 mL and transferred into an NMR tube; a $^1H$ NMR spectrum (−14.0 ppm) was obtained using $D_2O$/0.5 M $CH_3OH$ as both lock and external standard.

**[*fac*-$Ru(C_2H_5)(CO)_2(H_2O)_3]^+$ (5) and $[Ru_2(C_2H_5)_2(CO)_4(H_2O)_4][CF_3SO_3]_2$.** The triflato derivative of **4** (250 mL of a 0.04 M aqueous solution) was reacted for 1.5 h at 70 °C with 10 atm of ethene in a rocking stainless steel autoclave. Gases were vented, and the pale yellow solution, which showed carbonyl stretching bands at 2040 s and 1960 s $cm^{-1}$, was extracted for 24 h with refluxing $Et_2O$. Evaporation to dryness of the ether extract left 3.5 g (4.7 mmol, 94% yield) of a colorless solid, deliquescent in moist air and giving back large crystals of $[Ru_2(C_2H_5)_2(CO)_4(H_2O)_4][CF_3SO_3]_2$ in predried air. The molecular and crystal structures of the dinuclear $[Ru_2(C_2H_5)_2(CO)_4(H_2O)_4][CF_3SO_3]_2$ are reported in Figures 4 and 5, respectively. The crystalline solid (0.321 g, Ru 0.86 mmol) in 14.0 g of $H_2O$ caused a cryoscopic $\Delta T = 0.235$ °C. The IR spectrum of a 0.04 M solution of $[Ru_2(C_2H_5)_2(CO)_4(H_2O)_4][CF_3SO_3]_2$ showed absorptions at 2040 s and 1960 s $cm^{-1}$. $^1H$ NMR in $D_2O$: 1.16 (3H, t) and 1.74 ppm (2H, q).

**[*fac*-$Ru(C(O)C_2H_5)(CO)_2(H_2O)_3]^+$ (6).** The dinuclear crystalline $[Ru_2(C_2H_5)_2(CO)_4(H_2O)_4][CF_3SO_3]_2$ (0.372 g, 1.0 mmol of Ru) was dissolved in 25 g of $H_2O$ and reacted with CO in a gas-volumetric apparatus. Within 1 h at 30 °C, 25.9 mL of gas (0.99 mmol; CO/Ru molar ratio 0.99) was absorbed. At the end of the reaction the solution showed a cryoscopic $\Delta T = 0.152$ °C. IR of **6** 0.04 M in $H_2O$: $\nu_{CO}$ 2062 s and 1989 s $cm^{-1}$. $^1H$ NMR in $D_2O$: 0.83 (3H, t) and 2.77 ppm (2H, q). The gas-volumetric measurement, repeated in diglyme as solvent, was complete within minutes, and an equimolar amount of CO with respect to Ru was adsorbed.

**$Ru_4(C(O)C_2H_5)_4(OH)_2(CF_3SO_3)_2(CO)_8$ (7).** A 0.04 M solution (60 mL) of **6** as the triflate derivative was evaporated to dryness under vacuum and the residue dissolved in 30 mL of water-saturated $Et_2O$. Toluene (150 mL) was added and the solution concentrated until precipitation of a solid occurred. On standing overnight at −20 °C, colorless crystals of **7** were collected (0.64 g, 0.54 mmol, 90% yield). The molecular structure is shown in Figure 6. IR as poly(chlorotrifluoroethylene) mull: $\nu_{CO}$ 2069 s, 2023 s, 2010 vs, 2002 vs, and 1544 s $cm^{-1}$.

**X-ray Diffraction Study.** Crystals of **2** tetrafluoroborate derivative and of the dinuclear $[Ru_2(C_2H_5)_2(CO)_4(H_2O)_4][CF_3SO_3]_2$ were obtained by slow evaporation of their aqueous solutions. As both compounds are very soluble in water, very concentrated saturated solutions were obtained. In dry air, the solution solidified into a polycrystalline aggregate, which promptly redissolved upon exposure to moist air. Single crystals of diffractometric quality were prepared by careful admission of moist air. Once obtained, the crystals, which are hygroscopic, may be safely handled and sealed in glass capillaries in predried air.

All of the X-ray diffraction measurements were carried out with a Siemens P4 four-circle diffractometer, equipped with graphite-monochromatized Mo Kα radiation ($\lambda = 0.710\ 73$ Å). Low-temperature data collections were performed by cooling the crystal with a cold nitrogen gas stream obtained by a Siemens LT-2A device. All data collections were made in an $\omega/2\theta$ scan mode, collecting a redundant set of data in order to estimate their internal consistency. Three standard reflections were measured every 97 measurements, in order to monitor decay and equipment stability. Data reduction has been made by means of the XSCANS[9] program. Anisotropic thermal parameters were refined for all of the atoms except for hydrogens and disordered fluorines.

**Crystal Structure Determination of 1.** The crystals of **1** are colorless prisms defined by the forms {0 0 1}, {2 3 0}, {5 1 0}, and {1 $\bar{1}$ 0}. One of them was glued at the end of a glass fiber, mounted on the diffractometer, and cooled to 173 K. Cell parameters, calculated on the setting angles of 38 strong reflections having $\theta$ in the range 11.0−13.0°, are listed in Table 1. The Laue class of the diffraction pattern was recognized as 4/*m*. The intensity data were collected for a redundant set of reflections, with $\theta$ comprised between 1.87° and 29.98° in the range $-1 \le h \le 12$, $-1 \le k \le 12$, $-13 \le l \le 13$. A total of 2457 reflections were collected, corrected for Lorentz and polarization effects and for absorption by means of a Gaussian method.[10] After merging of the equivalent reflections ($R_{int} = [\Sigma|F_o^2 - F_o^2{}_{(mean)}|/\Sigma(F_o^2)] = 0.0202$), a set of 1903 unique reflections was obtained. The statistics on the normalized structure factors and the systematic absences suggested the tetragonal $P4_1$ or $P4_3$ as the most probable space group. The structure was solved in the $P4_1$ space group by an automatic Patterson method. Disorder in the position of the $CF_3$ groups was suggested by the electron density map. The disorder was interpreted as a statistical distribution of the trifluoroacetato groups in two different conformations, and two different $CF_3$ groups were introduced in each position, imposing the sums of occupancies to be equal to 1. One of the water hydrogens, H(1) in Figure 1, was localized in the difference Fourier map, while the position of the other was inferred from the position of the acceptor. The final refinement cycles were made using anisotropic thermal factors for Ru, O, and C atoms and isotropic for F atoms and imposing geometrical constraints to the $CF_3$ and $OH_2$ groups.

(8) Calderazzo, F.; Cotton, F. *Inorg. Chem.* **1962**, *1*, 30.

(9) *XSCANS, X-ray Single-Crystal Analysis System*, rel. 2.1; Siemens Analytical X-ray Instruments Inc.: Madison, WI, 1994.

(10) Sheldrick, G. M. SHELXTL-Plus, rel. 5.03; Siemens Analytical X-ray Instruments Inc.: Madison, WI, 1994.

**Table 1.** Crystal Data and Structure Refinement

| | **1** | **2** | $[Ru_2(C_2H_5)_2(CO)_4(H_2O)_4][CF_3SO_3]_2$ | **7** |
|---|---|---|---|---|
| empirical formula | $C_7H_2F_6O_8Ru$ | $C_3H_6B_2F_8O_6Ru$ | $C_{10}H_{18}F_6O_{14}Ru_2S_2$ | $C_{22}H_{22}F_6O_{20}Ru_4S_2$ |
| fw | 429.16 | 412.77 | 742.50 | 594.40 |
| temp, K | 173(2) | 173(2) | 173(2) | 293(2) |
| cryst syst, space group | tetragonal, $P4_1$ (No. 76) | trigonal, $R3$ (No. 146) | monoclinic, $P2_1/c$ (No. 14) | monoclinic, $P2_1/n$ (No. 14) |
| unit cell dimens | | | | |
| $a$, Å | 10.900(1) | 7.567(1) | 9.394(1) | 12.878(2) |
| $b$, Å | 10.900(1) | 7.567(1) | 15.679(3) | 11.561(2) |
| $c$, Å | 10.997(1) | 34.703(5) | 8.086(1) | 13.058(3) |
| α, deg | | 90 | | |
| $\beta$, deg | | 90 | 95.25(1) | 90.54(1) |
| $\gamma$, deg | | 120 | | |
| vol, Å$^3$ | 1306.6(2) | 1721.1(4) | 1186.0(3) | 1944.0(6) |
| $Z$ | 4 | 6 | 2 | 2 |
| $\rho_{calc}$, Mg/m$^3$ | 2.182 | 2.389 | 2.079 | 2.031 |
| $\mu$, mm$^{-1}$ | 1.314 | 1.499 | 1.557 | 1.733 |
| data/restraints/param | 1902/24/191 | 946/24/112 | 3009/0/160 | 2547/0/234 |
| $R(F_o)^a$ $[I > 2\sigma(I)]$ | 0.0424 | 0.0193 | 0.0385 | 0.0983 |
| $R_w{}^a$ $(F_o^2)$ $[I > 2\sigma(I)]$ | 0.1127 | 0.0483 | 0.0913 | 0.2519 |

[a] $R(F_o) = \sum||F_o| - |F_c||/\sum|F_o|$; $R_w(F_o^2) = [\sum[w(F_o^2 - F_c^2)^2]/\sum[w(F_o^2)^2]]^{1/2}$; $w = 1/[\sigma^2(F_o^2) + (AQ)^2 + BQ]$ where $Q = [MAX(F_o^2,0) + 2F_c^2]/3$.

The space group was verified by means of the enantiomorph-polarity parameter,[11] which was 0.03(9). The final reliability factors are listed in Table 1.

**Crystal Structure Determination of the Tetrafluoroborate Derivative of 2.** The crystals of **2** di-tetrafluoroborate are large hexagonal tables, dominated by the form {0 0 1}. A fragment of one of them, sealed in a glass capillary at room temperature, showed a trigonal lattice with unit cell parameters $a = 7.666(1)$ Å and $c = 34.983(5)$ Å. The collected intensities were corrected for Lorentz and polarization effects. The absorption correction was not applied owing to the relatively small dimensions of the crystal and the absence of good reflections suitable for $\psi$-scanning at $\chi$ angles near 90°. Systematic absences suggested the $R3$ (No. 146) or $R3m$ (No. 160) as the possible space group. The structure was solved in the more symmetric $R3m$ group by means of the automatic direct methods supported by the SIR92 program.[12] Two independent cationic moieties $[Ru(CO)_3(OH_2)_3]^{2+}$ and four $BF_4^-$ anions appeared to be placed all with the central atom on six $b$ Wyckoff positions. The cationic octahedra were consistent with the $3m$ site symmetry, but the anionic tetrahedra appeared to be rotated with respect to the $m$ plane so that double images were obtained. This can be explained either by a disorder of each anion on two different positions or by the absence of the $m$ plane (space group $R3$). Both possibilities were tried, but neither of them appeared to be better than the other, so we undertook a low-temperature measurement.

Another crystal was rapidly cut to a suitable size and fixed at the end of a glass fiber by means of a cyanoacrylic glue. It was mounted on the diffractometer and cooled to 173 K. Its unit cell volume decreased from 1780 Å$^3$ at room temperature to 1721 Å$^3$ at 173 K, but no phase transition was observed. The cell parameters, calculated from the setting angles of 15 accurately centered strong reflections with $2\theta$ ranging between 23.3° and 24.1°, at this temperature are listed in Table 1. The intensity data were collected till a $\theta_{max}$ of 30° in the index range $-1 \le h \le 10$, $-9 \le k \le 1$, $-1 \le l \le 48$. The 1182 collected intensities were corrected for Lorentz and polarization effects and for absorption by the empirical method contained in the XABS2 program.[13] After merging of the equivalent reflections, a set of 946 unique reflections was obtained ($R_{int} = 0.0444$). The refinement of the model obtained at room temperature in the $R3m$ space group gave less moving atoms, but still disordered anions. An observation, that disordered anions could hardly agree with the hydrogen interaction that fluorines and water ligands appeared to have, suggested to us the possibility that the $m$ plane resulted not from structure symmetry but from twinning. The final refinement cycles with twinning in the $R3$ space group removed the anion disorder and gave the reliability factors listed in Table 1.

**Crystal Structure Determination of $[Ru_2(C_2H_5)_2(CO)_4(H_2O)_4][CF_3SO_3]_2$.** Crystals grow as monoclinic tables dominated by the form {1 0 0}. Unit cell parameters determined on one of them sealed in a glass capillary at room temperature (292 K) were $a = 9.965(1)$ Å, $b = 16.073(2)$ Å, $c = 7.845(1)$ Å, $\alpha = 90°$, $\beta = 93.96(1)°$, $\gamma = 90°$. The diffraction showed $2/m$ symmetry, and the space group was recognized as $P2_1/c$. The crystal structure, determined on the intensity data collected at this temperature, showed the presence of disorder in the anions and did not allow the hydrogen atom positions to be localized. Thus, a measurement at low temperature was undertaken.

The crystal data determined at 173 K is listed in Table 1. No phase transition occurs between 292 and 173 K, and the cell volume decreased from 1253.5 to 1186.0 Å$^3$, the reduction being markedly anisotropic. As can be seen in Table 1, while $a$ and $b$ shorten by 5.7% and 2.5%, respectively, the $c$ axis grows by about 3%.

Intensities were collected between 2.18° and 30° of $\theta$, exploring the index ranges $-1 \le h \le 13$, $-22 \le k \le 1$, $-11 \le l \le 7$. A total of 3572 intensities were collected and corrected for Lorentz and polarization effects and for absorption by a Gaussian method based on the crystal faces. The structure was solved by standard statistical and Fourier methods by means of a SHELXTL program.[10] The hydrogen atoms were localized on the difference Fourier map, and the least-squares refinement gave the reliability factors listed in Table 1.

**Crystal Structure Determination of 7.** The crystals of **7** are monoclinic prisms. Some of them, sealed in glass capillaries, showed a diffraction pattern with $2/m$ symmetry; however, the diffraction was not sharp and the reflections appeared to be rather broad with indented profiles. As it was not possible to obtain better samples, the diffractometric analysis was undertaken; the unit cell parameters used in the following determination are listed in Table 1. Intensity data were measured only between 2.21° and 22.50° of $\theta$ because outside this range they dropped to unobservable values. The following index ranges were used: $-1 \le h \le 13$, $-12 \le k \le 1$, $-14 \le l \le 14$. A total of 3223 intensity data were collected and corrected for Lorentz and polarization effects. No absorption correction was applied owing to the limited quality of the data. The structure was solved by the standard statistical and Fourier methods, and hydrogen atoms were introduced in calculated positions. The H of the OH group was assumed to have a symmetric position with respect to the three ruthenium atoms. The resulting coordination of O(7) is approximately tetrahedral. The refinement procedure gave the final reliability factors listed in the last column of Table 1. The calculations were performed by means of the SHELXTL program.[10]

## Results and Discussion

Since the early work of Reppe[5] the relationship between water-gas shift reaction (WGSR) and olefin carbonylations with $CO/H_2O$ in alkaline solution was recognized, and the generali-

(11) Flack, H. D. *Acta Crystallogr*. **1983**, *A39*, 876.
(12) Altomare, A.; Burla, M. C.; Camalli, M.; Cascarano, G.; Giacovazzo, C.; Guagliardi, A.; Polidori G. *J. Appl. Crystallogr*. **1994**, *27*, 435.
(13) Parkin, S.; Moezzi, B.; Hope, H. *J. Appl. Crystallogr*. **1995**, *28*, 53.

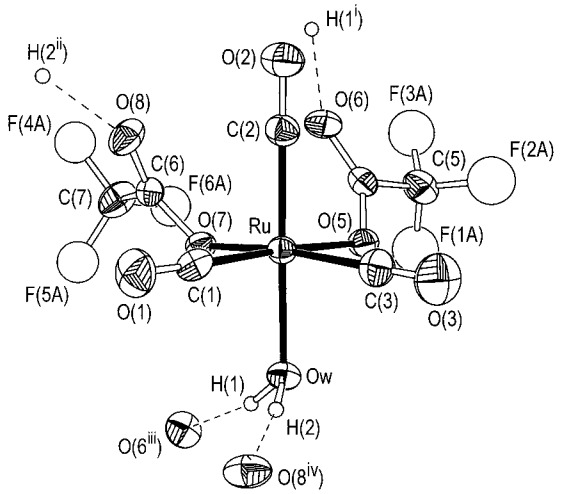


**Figure 1.** Molecular structure of [*fac*-Ru(OCOCF$_3$)$_2$(CO)$_3$(H$_2$O)] (**1**). Thermal ellipsoids are represented at 50% probability. The disordered fluorine atoms have been refined with isotropic thermal factors; for clarity they are represented in only one of the two possible positions, namely, that realized with the higher probability. The dashed lines represent the hydrogen interactions with the neighboring groups in the crystal. (i) = $-x$, $2 - y$, $-1/2 + z$; (ii) = $y$, $2 - x$, $-1/4 + z$; (iii) = $-x$, $2 - y$, $1/2 + z$; (iv) = $2 - y$, $x$, $1/4 + z$.

zation to other metal carbonyl derivatives was reported by Pettit.[14] From a mechanistic point of view, the attack by the strong nucleophile $OH^-$ to a CO ligand of a neutral metal carbonyl generates a hydridocarbonyl intermediate both for $H_2$ production in WGSR and for organic product formation in the presence of an olefin. At the onset of this work we investigated the olefin carbonylations supposedly related to the acid-cocatalyzed WGSR promoted by ruthenium carbonyls. Preliminary experiments showed that, upon admission of ethene into a $Ru_3(CO)_{12}$, $CF_3COOH$, diglyme, $H_2O$ solution during WGSR at 90 °C,[7] $H_2/CO_2$ production stops and no new catalytic processes begin. We regarded such a poisoning effect as an indication of water-soluble and stable organometallics generated by ethene interception of the Ru(II) hydrido carbonyl. The direct isolation and characterization of these organometallics, so exceptionally inert at 90 °C in the presence of $H_2O$ and acids, was discouraged by the complexity of IR and NMR spectra of the poisoned WGSR solution. As matter of fact, these spectra appeared crowded, the reason for this being the competition by diglyme, $CF_3COO^-$, and $H_2O$ for the coordination sphere of ruthenium(II), as shown in the next paragraph. Then, we attempted to obtain the Ru(II) hydrido carbonyl intermediate with $H_2O$ only as coligand and its reaction with ethene was studied in water. The synthesis of [*fac*-RuH(CO)$_2$(H$_2$O)$_3$]$^+$ (**4**) was thus performed starting from *fac*-Ru(OCOCF$_3$)$_2$(CO)$_3$[(CH$_3$)$_2$CHOH].[7]

**Isolation, Molecular Structure, and Behavior in $H_2O$ of *fac*-Ru(OCOCF$_3$)$_2$(CO)$_3$(H$_2$O) (1).** Complex **1** was obtained by substitution reaction by $H_2O$ of the 2-propanol ligand of *fac*-Ru(OCOCF$_3$)$_2$(CO)$_3$(*i*-PrOH). The ligand exchange cannot be carried out in aqueous solution where the 2-propanol complex is sparingly soluble and a slow substitution reaction is accompanied by nucleophilic attack by water at the CO ligands. A convenient method for the synthesis of **1** consists of dissolving *fac*-Ru(OCOCF$_3$)$_2$(CO)$_3$(*i*-PrOH) in water-saturated Et$_2$O and evaporating the solution to dryness. A projection of the molecular structure of **1** is shown in Figure 1, bond distances and angles being listed in Table 2. The coordination geometry at ruthenium is slightly distorted octahedral, and the three carbonyl groups are arranged facially. The distortion is mainly due to the tilting of both Ru−O(5) and Ru−O(7) bonds toward the coordinated water.

**Table 2.** Main Bond Lengths (Å) and Angles (deg) for **1**

| | | | |
|---|---|---|---|
| Ru−C(1) | 1.899(8) | C(3)−O(3) | 1.115(11) |
| Ru−C(2) | 1.921(8) | O(5)−C(4) | 1.275(10) |
| Ru−C(3) | 1.923(9) | C(4)−O(6) | 1.211(11) |
| Ru−O(7) | 2.058(6) | C(4)−C(5) | 1.576(11) |
| Ru−O(5) | 2.077(5) | O(7)−C(6) | 1.274(10) |
| Ru−Ow | 2.097(6) | C(6)−O(8) | 1.224(10) |
| C(1)−O(1) | 1.132(11) | C(6)−C(7) | 1.561(10) |
| C(2)−O(2) | 1.113(12) | | |
| C(1)−Ru−C(2) | 89.3(3) | O(7)−Ru−Ow | 82.9(2) |
| C(1)−Ru−C(3) | 93.2(4) | O(5)−Ru−Ow | 83.2(2) |
| C(2)−Ru−C(3) | 90.7(4) | O(1)−C(1)−Ru | 177.4(7) |
| C(1)−Ru−O(7) | 93.4(3) | O(2)−C(2)−Ru | 175.9(7) |
| C(2)−Ru−O(7) | 96.2(3) | O(3)−C(3)−Ru | 178.3(8) |
| C(3)−Ru−O(7) | 170.5(3) | C(4)−O(5)−Ru | 118.4(5) |
| C(1)−Ru−O(5) | 175.4(3) | O(6)−C(4)−O(5) | 128.7(8) |
| C(2)−Ru−O(5) | 94.5(3) | O(6)−C(4)−C(5) | 118.7(7) |
| C(3)−Ru−O(5) | 89.3(3) | O(5)−C(4)−C(5) | 112.7(7) |
| O(7)−Ru−O(5) | 83.6(2) | C(6)−O(7)−Ru | 124.3(6) |
| C(1)−Ru−Ow | 93.0(3) | O(8)−C(6)−O(7) | 128.6(8) |
| C(2)−Ru−Ow | 177.6(3) | O(8)−C(6)−C(7) | 120.3(7) |
| C(3)−Ru−Ow | 89.9(3) | O(7)−C(6)−C(7) | 111.1(7) |

The Ru−CO distances (mean value 1.914 Å) are in keeping with the value of 1.90(4) Å, obtained by averaging 1453 Ru−C distances observed in Ru(II) carbonyl derivatives.[15] The water molecule binds to the metal at 2.097 Å; this value may be regarded as the lower limit of ruthenium(II)−water distances, as the range till now observed spans between 2.105(4) Å in $RuCl_2(CO)_3(H_2O)$·diglyme[16] and 2.202(6) Å in Ru(*p*-toluenesulfonato)$_2$(CO)(H$_2$O)(P(C$_6$H$_5$)$_3$)$_2$.[17] The molecular structure of **1** can be compared to that of the analogous $Ru(CO)_3Cl_2H_2O$·diglyme. In this latter compound, the mandatory hydrogen bonds of coordinated water in the crystal involve diglyme as hydrogen bond acceptor while in **1** the trifluoroacetato ligands perform this role. The Ow···O distances in **1** for the hydrogen-bonded trifluoroacetato groups are both 2.66 Å, a value near the lower limit of H-bonded O···O distances, 2.6 Å,[18] suggestive of a strong interaction. Each molecule of **1** behaves as an acceptor of two hydrogen bonds and as a donor of two others, as shown in Figure 1, thus forming a tridimensional network of connected molecules. These structural parameters together with the high CO stretching frequences[19] ($\nu_{CO}$ = 2153 s, 2094 vs, and 2079 vs cm$^{-1}$, Nujol mull) indicate a strong degree of activation of the CO ligands toward nucleophilic attack and anticipate the acidic character of coordinated $H_2O$.[20]

Complex **1** is quite soluble in an acidic aqueous solution where the nucleophilic attack by the solvent onto its CO ligands is prevented and complexes of the series [*fac*-Ru(OCOCF$_3$)$_n$(CO)$_3$(H$_2$O)$_m$]$^{(2-n)+}$ ($n + m = 3$) are formed. As a matter of fact, the IR spectrum of **1** in 0.5 M $CF_3COOH$ shows two broad

(14) Kang, H.; Mauldin, C. H.; Cole, T.; Slegeir, W.; Cann, K.; Pettit, R. *J. Am. Chem. Soc.* **1977**, *99*, 8323.
(15) Orpen, A. G.; Brammer, L.; Allen, F. H.; Kennard, O.; Watson, D. G.; Taylor, R. *J. Chem. Soc., Dalton Trans.* **1989**, S1.
(16) Bergmeister, J. J., III; Hanson, B. E.; Merola, J. S. *Inorg. Chem.* **1990**, *29*, 4831.
(17) Harding, P. A.; Robinson, S. D.; Henrick, K. *J. Chem. Soc., Dalton Trans.* **1988**, 415.
(18) Ferraris, G.; Franchini-Angela, M. *Acta Crystallogr.* **1972**, *B28*, 3572.
(19) (a) Darensbourg, D. J.; Darensbourg, M. Y. *Inorg. Chem.* **1970**, *9*, 1691. (b) Johnston, G. G.; Hommeltoft, S. I.; Baird, M. C. *Organometallics* **1989**, *8*, 1904. (c) Bao, Q. B.; Rheingold, A. L.; Brill, T. B. *Organometallics* **1986**, *5*, 2259.
(20) Stanko, J. A.; Chaipayungpundhu, S. *J. Am. Chem. Soc.* **1970**, *92*, 5580.

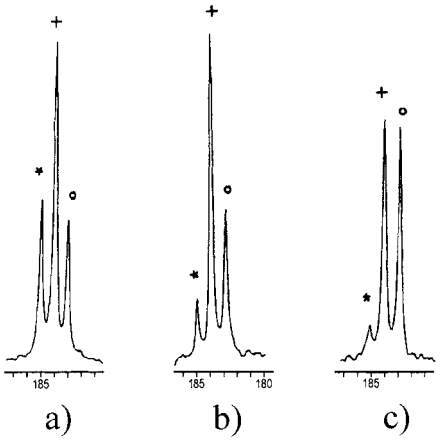


**Figure 2.** $^{13}C$ NMR spectra of a 0.03 M solution of $^{13}CO$-enriched **1**: (a) same spectrum in $D_2O$/0.5 M $CF_3COOH$ or on adding $CF_3COOK$ 0.5 M to the solution in part c; (b) in $D_2O$/0.5 M $HBF_4$; (c) in $D_2O$/1.0 M $HBF_4$; (∗) *fac*-$Ru(OCOCF_3)_2(CO)_3(H_2O)$; (+) [*fac*-$Ru(OCOCF_3)(CO)_3(H_2O)_2]^+$; (∘) [*fac*-$Ru(CO)_3(H_2O)_3]^{2+}$.

absorptions ($\nu_{CO}$ = 2152 s and 2088 vs $cm^{-1}$), while the $^{13}C$ NMR spectrum of a $^{13}CO$-enriched sample of **1** in $D_2O$/0.5 M $CF_3COOH$ displays three resonances at 183.0, 184.0, and 184.8 ppm. In 0.5 M $HBF_4$, only minor modifications occur in the IR spectrum. In $D_2O/HBF_4$, however, the $^{13}C$ NMR spectrum of a $^{13}CO$-enriched sample of **1** reveals that the resonance at 184.8 ppm decreases in favor of that at 183.0 ppm (Figure 2). The intensity of the three resonances can be restored by adding $CF_3COOK$.

These findings indicate that the strong acid $HBF_4$ protonates the $CF_3COO^-$ ligands and that the 183.0, 184.0, and 184.8 ppm resonances can be attributed to the $n = 0$, $n = 1$, and $n = 2$ members, respectively, of the above series. The $n = 3$ anionic complex, whose structure has already been presented,[7] can only be detected when its precipitation occurs on addition of an excess of $CF_3COOCs$. Such an interpretation of the spectroscopic properties of **1** in acidic solutions anticipates the existence of $[Ru(CO)_3(H_2O)_3]^{2+}$ (**2**) and indicates a suitable method for its synthesis consisting of treating **1** with a strong acid whose conjugate base is weakly coordinating.

**Behavior in $H_2O$ solution of [*fac*-$Ru(CO)_3(H_2O)_3]^{2+}$ (2) and Isolation and Molecular Structure of the Tetrafluoroborate Derivative.** The synthesis of **2** was achieved by treating **1** with $HBF_4$ or $CF_3SO_3H$. The tetrafluoroborate derivative of **2** was isolated in pure form as an air-stable colorless deliquescent solid. Figure 3 shows the molecular structure of the cation, and Table 3 lists the bond distances and angles.

The asymmetric unit contains two independent $[Ru(CO)_3(H_2O)_3]^{2+}$ cations, both placed on the trigonal axis. The coordination geometry around ruthenium may be regarded as octahedral, distorted toward trigonal antiprism, with the three water ligands in *fac* position. The Ow−Ru−C angles of nearly 95° elongate the octahedron in the *c* direction toward the antiprism. The Ru−CO and Ru−Ow bond distances are usual for Ru(II) complexes, although the latter is near the lower limit of the range. An extended network of hydrogen bonds, involving the coordinated water and some fluorines of the anions, arranges the crystal structure in layers parallel to the (0 0 1) plane, such that they are the principal faces of the crystal. Two layers of thickness *c*/2 (17.35 Å) are present in the unit cell. The interactions present in such layers are similar to those described in more detail for the dinuclear triflate derivative $[Ru_2(C_2H_5)_2(CO)_4(H_2O)_4][CF_3SO_3]_2$ (see below). As far as we know, there

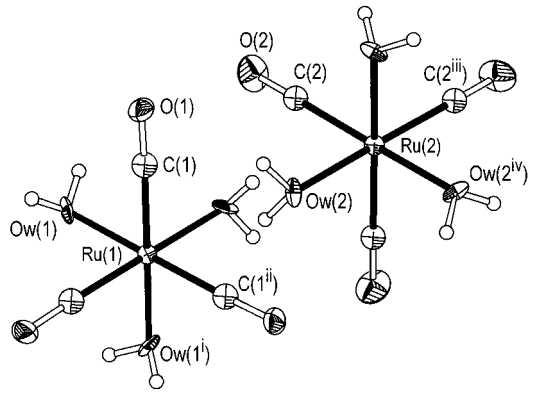


**Figure 3.** Molecular structure of the two independent cations $[Ru(CO)_3(H_2O)_3]^{2+}$ (**2**) projected along the *c* axis. The ellipsoids are at 50% probability. (i) = $1 - y, x - y, z$; (ii) = $1 + y - x, 1 - x, z$; (iii) = $y - x, 1 - x, z$; (iv) = $1 - y, 1 + x - y, z$.

**Table 3.** Bond Lengths (Å) and Angles (deg) for **2** Di-tetrafluoroborate[a]

| | | | |
|---|---|---|---|
| Ru(1)−C(1) | 1.920(5) | Ru(2)−C(2) | 1.925(4) |
| Ru(1)−Ow(1) | 2.100(5) | Ru(2)−Ow(2) | 2.126(4) |
| C(1)−O(1) | 1.121(5) | C(2)−O(2) | 1.107(5) |
| Ow(1)−Ru(1)−Ow(1i) | 81.4(3) | Ow(2)−Ru(2)−Ow(2iii) | 82.6(3) |
| Ow(1)−Ru(1)−C(1) | 94.9(3) | Ow(2)−Ru(2)−C(2) | 93.5(3) |
| Ow(1)−Ru(1)−C(1i) | 95.5(4) | Ow(2)−Ru(2)−C(2iv) | 92.4(4) |
| Ow(1)−Ru(1)−C(1ii) | 175.4(4) | Ow(2)−Ru(2)−C(2iii) | 174.0(4) |
| C(1)−Ru(1)−C(1ii) | 88.1(4) | C(2)−Ru(2)−C(2iii) | 91.1(4) |
| Ru(1)−C(1)−O(1) | 174.7(9) | Ru(2)−C(2)−O(2) | 175.2(10) |

[a] The apexes in the atom labels have the same meaning as in Figure 3.

are only four more examples, not yet structurally characterized, of metal carbonyls with only $H_2O$ as coligand, namely, $[Ru(CO)(H_2O)_5]^{2+}$,[21] $[Re(CO)_5(H_2O)]^+$,[22] $[Re(CO)_3(H_2O)_3]^+$,[23] and $[Tc(CO)_3(H_2O)_3]^+$.[24]

With respect to these, the dicationic tricarbonyl **2** was anticipated to be more susceptible to nucleophilic attack by water. As a matter of fact, **2** exists exclusively in the solid state and in strongly acidic solution. The IR spectra of **2** in the solid state ($\nu_{CO}$: 2181 s and 2122 vs $cm^{-1}$, Nujol mull) and in $D_2O$/0.5 M $HBF_4$ ($\nu_{CO}$: 2160 s and 2095 vs $cm^{-1}$) are similar, and both do not show absorptions in the 1700−1500 $cm^{-1}$ region. The $^{13}C$ NMR spectrum of a $^{13}CO$-enriched sample of **2** in $D_2O$/0.5 M $HBF_4$ displays a unique resonance at 183.0 ppm.

In aqueous solution, **2** itself is acidic with a pH value of 1.6 in a 0.04 M solution. Such a partial deprotonation of **2** corresponds to the formation of a ruthenacarboxylic acid carrying two *cis*-CO groups and, presumably, three $H_2O$ groups as coligands, see Scheme 1. As a matter of fact, the IR spectrum of a freshly prepared 0.04 M solution of **2** shows three new bands accompanying the absorptions of **2**: those at 2075 vs and 2004 vs $cm^{-1}$ can be attributed to the *cis*-$Ru(CO)_2$ grouping while that at 1616 m $cm^{-1}$ ($D_2O$ solution) can be attributed to RuC(O)OD. Also the $^{13}C$ NMR spectrum of a $^{13}CO$-enriched sample of **2** in $D_2O$ shows new resonances together with the

(21) Laurenczy, G.; Helm, L.; Ludi, A.; Merbach, A. E. *Helv. Chim. Acta* **1991**, *74*, 1236.
(22) Raab, K.; Olgemoeller, B.; Schloter, K.; Beck, W. J. *J. Organomet. Chem.* **1981**, *214*, 81.
(23) Alberto, R.; Egli, A.; Abram, U.; Hegetschweiler, K.; Gramlich, V.; Schubiger, P. A. *J. Chem. Soc., Dalton Trans.* **1994**, 2815.
(24) Alberto, R.; Egli, A.; Schibli, R.; Schaffland, A.; Abram, U.; Kaden, T. A.; Schubiger, A. P. Presented at the XXXIII International Conference on Coordination Chemistry, Aug 31−Sept 4, 1998, Florence.

**Scheme 1.** Fast pH-Dependent Equilibrium between **2** and the Ruthenacarboxylic Acid, the Latter Slowly Forming **4**

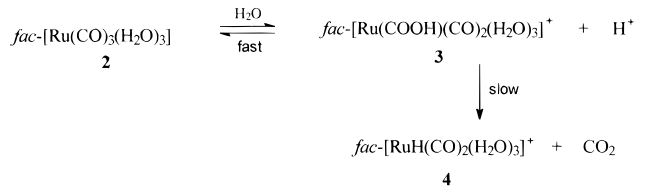


183.0 ppm resonance of undissociated **2**. On addition of $HBF_4$, **2** is quantitatively and immediately restored, as shown by the IR and NMR spectra. On these grounds, it appears that **2** and the metallacarboxylic acid arising from nucleophilic attack by $H_2O$ onto its activated CO ligands coexist in a pH-controlled fast equilibrium.

**Formation and Properties of [*fac*-RuH(CO)$_2$(H$_2$O)$_3$]$^+$ (4) in H$_2$O.** Solutions in which the fast equilibrium of Scheme 1 operates are of moderate stability as $CO_2$ elimination from the ruthenacarboxylic acid occurs. At room temperature, the IR absorptions of both **2** and the ruthenacarboxylic acid are converted into two new absorptions at lower frequencies (2053 s and 1973 s $cm^{-1}$) while also the 2343 $cm^{-1}$ band of $CO_2$ becomes evident. The reaction is complete within 3 h as indicated by IR spectroscopy and quantitative $CO_2$ determinations. $^1$H NMR analysis of the solution finally shows a unique resonance at $-14.0$ ppm,[25] which, together with the IR absorptions attributable to a *cis*-Ru(CO)$_2$ grouping, reveals the formation of **4**. Potentiometric titration curves of the solution where **4** is generated from **2** display two pH jumps at 1.0 and 2.0 equiv of added base. The former corresponds to the titration of the strong acid accompanying **4** (Scheme 1), while the latter documents the weakly acid character of **4** ($pK_a = 5$).

**Formation of [*fac*-Ru(C$_2$H$_5$)(CO)$_2$(H$_2$O)$_3$]$^+$ (5) in H$_2$O. Isolation and Crystal and Molecular Structure of the Dinuclear [Ru$_2$(C$_2$H$_5$)$_2$(CO)$_4$(H$_2$O)$_4$][CF$_3$SO$_3$]$_2$.** The 0.04 M solution of both **4** and $CF_3SO_3H$ as obtained from the decomposition of **2** triflate derivative was reacted with ethene at 70 °C under a pressure of 10 atm. Continuous extraction with $Et_2O$ and evaporation to dryness of the extract leaves a colorless residue which deliquesces in moist air and gives large crystals in dry air. As in the recently reported case of ethyl(dicarbonyl)(chloro)ruthenium dimer[26] also the cationic **5** is dinuclear in the solid state. The molecular structure of $[Ru_2(C_2H_5)_2(CO)_4(H_2O)_4]^{2+}$ is shown in Figure 4. Bond distances and angles are listed in Table 4.

The cation consists of two distorted octahedra [*fac*-Ru(C$_2$H$_5$)(CO)$_2$(H$_2$O)$_3$]$^+$ joined by sharing one edge with bridging water groups. The bridging ligands, however, are not equally shared by the two metal atoms, the Ru−Ow(1) bond length being 2.365(3) Å, while Ru−Ow(1$^i$) is 2.185(3) Å. Two very short Ru−CO distances (1.84 Å) are present which agree with the CO stretchings observed at the lowest $\nu$ among our compounds. In the crystal, $[Ru_2(C_2H_5)_2(CO)_4(H_2O)_4][CF_3SO_3]_2$ has a layer structure. The layers are kept together by weak van der Waals interactions and are characterized by hydrophobic−hydrophilic interactions. A scheme is shown in Figure 5. The layer, 9.39 Å thick, is made by an intermediate hydrophilic wafer containing the water ligands, the Ru atoms and the $SO_3$ groups of the triflate being embedded between two hydrophobic coats, formed by CO, $CF_3$, and $C_2H_5$ groups. In aqueous solution the dinuclear cation is converted into the mononuclear [*fac*-Ru(C$_2$H$_5$)(CO)$_2$(H$_2$O)$_3$]$^+$ (**5**) as shown by cryoscopy in water. In water **5** is among the most inert alkyl complexes: **5**, 0.04 M in $H_2O$, is unaffected by strong acids and remains unchanged for days in air, daylight and for hours in boiling water. In diglyme, however, it decomposes at 90 °C, forming ethane and ethene. **5** inserts CO at room temperature and atmospheric pressure both in water and in diglyme solution. Rate measurements of gas uptake show that in diglyme the rate is diffusion-controlled while in water 1 h is required for the reaction to be complete at room temperature.

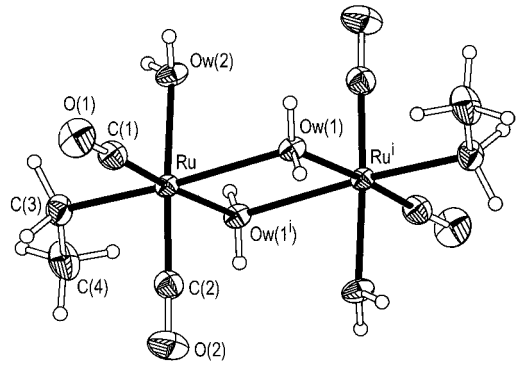


**Figure 4.** View of the molecular structure of $[Ru_2(C_2H_5)_2(CO)_4(H_2O)_4]^{2+}$. Thermal ellipsoids are at 50% probability. (i) $= -x, 2 - y, -z$.

**Table 4.** Bond Lengths (Å) and Angles (deg) for Dinuclear $[Ru_2(C_2H_5)_2(CO)_4(H_2O)_4]$ $[CF_3SO_3]_2$

| | | | |
|---|---|---|---|
| Ru−C(1) | 1.846(5) | C(3)−C(4) | 1.507(6) |
| Ru−C(2) | 1.848(4) | S−O(5) | 1.444(3) |
| Ru−C(3) | 2.100(4) | S−O(4) | 1.444(3) |
| Ru−Ow(2) | 2.149(3) | S−O(3) | 1.452(3) |
| Ru−Ow(1′) | 2.185(3) | S−C(5) | 1.832(5) |
| Ru−Ow(1) | 2.365(3) | C(5)−F(1) | 1.302(7) |
| C(1)−O(1) | 1.133(6) | C(5)−F(3) | 1.301(6) |
| C(2)−O(2) | 1.140(5) | C(5)−F(2) | 1.320(7) |

| | | | |
|---|---|---|---|
| C(1)−Ru−C(2) | 87.7(2) | C(1)−Ru−Ow(1) | 99.7(1) |
| C(1)−Ru−C(3) | 86.4(2) | C(2)−Ru−Ow(1) | 97.3(1) |
| C(2)−Ru−C(3) | 89.6(2) | C(3)−Ru−Ow(1) | 170.9(2) |
| C(1)−Ru−Ow(2) | 96.5(2) | Ow(2)−Ru−Ow(1) | 80.9(1) |
| C(2)−Ru−Ow(2) | 175.6(2) | Ow(1$^i$)−Ru−Ow(1) | 76.6(1) |
| C(3)−Ru−Ow(2) | 91.8(2) | Ru$^i$−OW(1)−Ru | 103.4(1) |
| C(1)−Ru−Ow(1$^i$) | 175.8(1) | O(1)−C(1)−Ru | 177.6(4) |
| C(2)−Ru−Ow(1$^i$) | 94.6(2) | O(2)−C(2)−Ru | 178.4(4) |
| C(3)−Ru−Ow(1$^i$) | 97.1(1) | C(4)−C(3)−Ru | 113.7(3) |
| Ow(2)−Ru−Ow(1$^i$) | 81.1(1) | | |

[a] The apexes in the atom labels have the same meaning as in Figure 4.

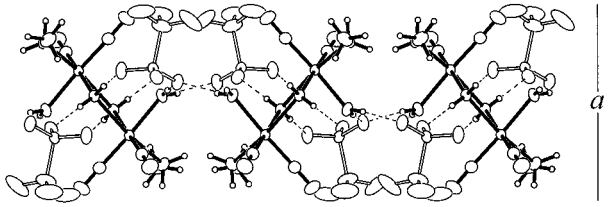


**Figure 5.** View of a layer in the crystal structure of the dinuclear $[Ru_2(C_2H_5)_2(CO)_4(H_2O)_4][CF_3SO_3]_2$ projected down the *c* axis. Bonds within the cations are drawn with solid full lines. The water molecules are embedded within the layer and interact (dashed lines) with the anions.

**Reaction of [*fac*-Ru(C$_2$H$_5$)(CO)$_2$(H$_2$O)$_3$]$^+$ (5) with CO in H$_2$O. Isolation and Structure of Ru$_4$(C(O)C$_2$H$_5$)$_4$(OH)$_2$(CF$_3$SO$_3$)$_2$(CO)$_8$ (7).** Gas-volumetric measurements show that **5**, 0.04 M in $H_2O$, absorbs an equimolar amount of CO. Freezing point depression of an aqueous solution of **5** remains unchanged

(25) Kaesz, H. D.; Saillant, R. B. *Chem. Rev.* **1972**, *72*, 231.
(26) Fabre, S.; Kalck, P.; Lavigne, G. *Angew. Chem., Int. Ed. Engl.* **1997**, *36*, 1092.

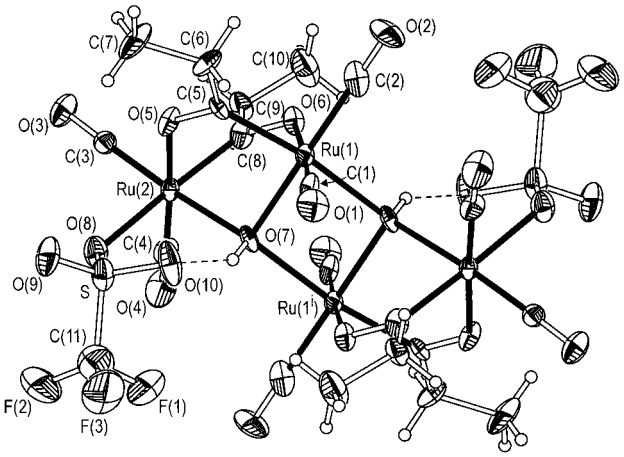


**Figure 6.** Molecular structure of **7**. Thermal ellipsoids are at 30% probability. Coordination around the metal is evidenced by solid full lines. Dashes represent the hydrogen interactions. (i) = $1-x, -y, 1-z$.

after the reaction with CO, thus indicating the mononuclear nature of the cationic product. Removal under vacuum of the aqueous solvent at the end of the CO absorption leaves a colorless residue of [*fac*-$Ru(C(O)C_2H_5)(CO)_2(H_2O)_3][CF_3SO_3]$ (**6**) ($^1$H NMR in $D_2O$: 0.83 (3H, t) and 2.77 ppm (2H, q). IR in $H_2O$: $\nu_{CO}$ 2062 s and 1989 s cm$^{-1}$). Attempts to recrystallize **6** from organic solvents resulted in triflic acid release and formation of the tetranuclear complex **7** according to eq 1.

$$4[\textit{fac}\text{-}Ru(C(O)C_2H_5)(CO)_2(H_2O)_3][CF_3SO_3] \xrightarrow[-2CF_3SO_3H]{Et_2O} \underset{\mathbf{7}}{Ru_4(C(O)C_2H_5)_4(OH)_2(CF_3SO_3)_2(CO)_8} \quad (1)$$
**6**

Because of the poor quality of the crystals, the molecular structure of **7** has not been determined with the same accuracy as for the other compounds reported in this paper. However, atom connectivity was established and the structure is briefly discussed. Figure 6 displays a projection of the tetranuclear molecule, and its bond distances and angles are listed in Table 5. The whole molecule is obtained by the operation of an inversion center $\bar{1}$ on the asymmetric unit $\{Ru_2(COC_2H_5)_2(CO)_4(OH)(OSO_2CF_3)\}$. Two octahedral $\{Ru(CO)_2(OH)_2(OCC_2H_5)(COC_2H_5)\}$ units are connected by sharing the edge bearing the OH groups. Each OH group is furthermore shared by another dicarbonyl triflate ruthenium octahedron, which completes its coordination by binding to bridging acyl ligands of one ruthenium atom of the first pair. The triflato ligand confirms its weak binding ability, making a much longer bond with Ru(2) (2.30 Å) than, for instance, that formed by the trifluoroacetato in compound **1** (Ru−O 2.06 Å). Two strong intramolecular hydrogen bonds are formed among hydroxyl groups and two uncoordinated oxygens of the triflates (O(7)···O(10) 2.674 Å). The presence of bidentate acyl ligands together with tricoordinated OH groups has already been observed in the hexanuclear $[Ru_3Cl_3(COC_2H_5)_2(OH)(CO)_6]_2 \cdot C_6H_6$.[27] Bond lengths and angles involving OH and acyl groups are very similar in such two ruthenium derivatives.

**Elimination of Propionic Acid from [*fac*-$Ru(C(O)C_2H_5)(CO)_2(H_2O)_3]^+$.** The effect of water as coligand and solvent allows a privileged observation of the fundamental steps in olefin activation. At higher temperature, however, a catalytic cycle is observed producing propionic acid from ethene CO and $H_2O$ (Scheme 2) in fully aqueous solvent.

Preliminary observations show that the catalytic formation of propionic acid is inhibited by high $P_{CO}$ and cocatalyzed by

(27) Merlino, S.; Montagnoli, G.; Braca, G.; Sbrana, G. *Inorg. Chim. Acta* **1978**, *27*, 233.

**Table 5.** Selected Bond Lengths (Å) and Angles (deg) for **7**[a]

| | | | |
|---|---|---|---|
| Ru(1)−C(2) | 1.88(3) | Ru(2)−O(8) | 2.30(2) |
| Ru(1)−C(1) | 1.90(2) | C(1)−O(1) | 1.10(2) |
| Ru(1)−C(5) | 2.00(2) | C(2)−O(2) | 1.11(3) |
| Ru(1)−O(6) | 2.12(1) | C(3)−O(3) | 1.19(2) |
| Ru(1)−O(7) | 2.12(1) | C(4)−O(4) | 1.12(3) |
| Ru(1$^i$)−O(7) | 2.28(1) | O(5)−C(5) | 1.24(2) |
| Ru(2)−C(3) | 1.81(2) | C(5)−C(6) | 1.48(3) |
| Ru(2)−C(4) | 1.87(2) | C(6)−C(7) | 1.51(3) |
| Ru(2)−C(8) | 1.96(2) | O(6)−C(8) | 1.25(2) |
| Ru(2)−O(5) | 2.11(1) | C(8)−C(9) | 1.52(3) |
| Ru(2)−O(7) | 2.14(1) | C(9)−C(10) | 1.54(3) |
| C(2)−Ru(1)−C(1) | 91.2(9) | C(8)−Ru(2)−O(7) | 86.0(7) |
| C(2)−Ru(1)−C(5) | 92.0(9) | O(5)−Ru(2)−O(7) | 84.8(5) |
| C(1)−Ru(1)−C(5) | 88.0(8) | C(3)−Ru(2)−O(8) | 95.2(7) |
| C(2)−Ru(1)−O(6) | 91.5(8) | C(4)−Ru(2)−O(8) | 93.0(8) |
| C(1)−Ru(1)−O(6) | 176.5(7) | C(8)−Ru(2)−O(8) | 170.2(7) |
| C(5)−Ru(1)−O(6) | 89.6(7) | O(5)−Ru(2)−O(8) | 84.4(6) |
| C(2)−Ru(1)−O(7) | 173.0(7) | O(7)−Ru(2)−O(8) | 86.8(5) |
| C(1)−Ru(1)−O(7) | 95.5(7) | O(1)−C(1)−Ru(1) | 178(2) |
| C(5)−Ru(1)−O(7) | 90.3(6) | O(2)−C(2)−Ru(1) | 179(2) |
| O(6)−Ru(1)−O(7) | 81.9(5) | O(3)−C(3)−Ru(2) | 178(2) |
| C(2)−Ru(1)−O(7$^i$) | 97.8(8) | O(4)−C(4)−Ru(2) | 177(2) |
| C(1)−Ru(1)−O(7$^i$) | 98.6(7) | C(5)−O(5)−Ru(2) | 124.1(13) |
| C(5)−Ru(1)−O(7$^i$) | 168.0(6) | O(5)−C(5)−C(6) | 116(2) |
| O(6)−Ru(1)−O(7$^i$) | 83.3(5) | O(5)−C(5)−Ru(1) | 116.3(14) |
| O(7)−Ru(1)−O(7$^i$) | 79.2(5) | C(6)−C(5)−Ru(1) | 127.4(14) |
| C(3)−Ru(2)−C(4) | 86.7(9) | C(8)−O(6)−Ru(1) | 120.6(14) |
| C(3)−Ru(2)−C(8) | 91.7(9) | O(6)−C(8)−C(9) | 114(2) |
| C(4)−Ru(2)−C(8) | 94.4(9) | O(6)−C(8)−Ru(2) | 120.0(15) |
| C(3)−Ru(2)−O(5) | 91.8(7) | C(9)−C(8)−Ru(2) | 125.7(14) |
| C(4)−Ru(2)−O(5) | 176.9(8) | Ru(1)−O(7)−Ru(2) | 102.0(6) |
| C(8)−Ru(2)−O(5) | 88.4(7) | Ru(1)−O(7)−Ru(1$^i$) | 100.8(5) |
| C(3)−Ru(2)−O(7) | 175.9(7) | Ru(2)−O(7)−Ru(1$^i$) | 126.3(5) |
| C(4)−Ru(2)−O(7) | 96.8(7) | | |

[a] The apex in the atom label has the same meaning as in Figure 6.

**Scheme 2.** Aqueous Organometallic Chemistry of Ru(II) Aquocarbonyl Complexes and Mechanism of the High-Temperature Ethene Hydrocarboxylation in Fully Aqueous Solvent

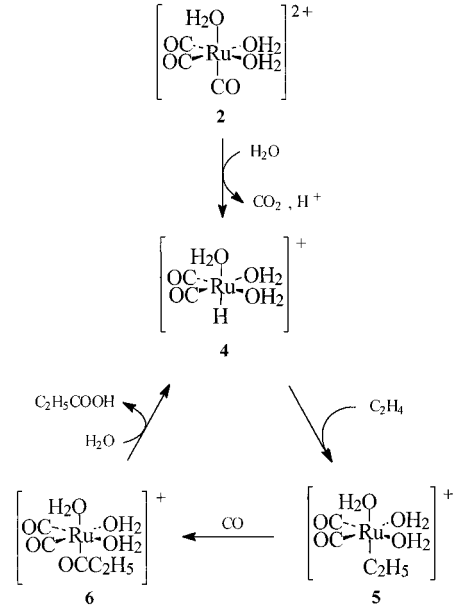

strong acids: a TOF($C_2H_5COOH$) = 15.4 (TOF($C_2H_5COOH$) = moles of $C_2H_5COOH$/moles of Ru/h)) was observed for a 0.01 M solution of **6**, $P_{CO}$ = 4 atm, $P_{ethene}$ = 30 atm, [$CF_3SO_3H$] = 0.1 M, and $T$ = 140 °C. The IR analysis of samples withdrawn during the catalytic process reveals the concentration of **6** to be unchanged, thus suggesting the elimination of carboxylic acid as the slow step of such a hydrocarboxylation in a fully aqueous solvent. The propionic acid produced affects the selectivity of the process. As a matter of fact, a reductive hydrocarbonylation of ethene to diethyl ketone according to eq 2 accompanies hydrocarboxylation when [$C_2H_5COOH$] > 3 M.

$$2C_2H_4 + 2CO + H_2O \rightarrow C_2H_5C(O)C_2H_5 + CO_2 \quad (2)$$

A more detailed study of the catalytic properties in aqueous solution of the Ru(II) organometallic derivatives of Scheme 2 will appear in a forthcoming paper.

## Conclusions

Aqueous organometallic chemistry can have numerous applications.[1] The findings of this paper could encourage research in this field: water as coligand allows the synthesis of organometallics stable in water. The strong coordinating power of water and the extra stability due to the net of hydrogen bonds with bulk water make these aquo organometallic complexes inert by hindering the formation of vacant sites. Thus, we have been able to document on the same system the complete sequence of fundamental reactions as required for olefin activation. As an application, the Reppe-type olefin hydrocarboxylation and hydrocarbonylation catalytic reactions become processes feasible in fully aqueous solvent. Finally, the accumulation of complex **6** during the catalytic process and the persistence of this exotic substance in water suggest that the widely expected environmental advantages of the industrial application of water as a solvent for industrial organic chemistry must be reconsidered.

**Acknowledgment.** We thank Prof. F. Calderazzo and Prof. S. Merlino for helpful discussions, Mr. F. Del Cima for skillful technical assistance, Chimet SpA for a gift of ruthenium, and Ministero della Ricerca Scientifica e Tecnologica (MURST) Programmi di Ricerca Scientifica di Rilevante Interesse Nazionale, Cofinanziamento 1998−1999.

**Supporting Information Available:** X-ray crystallographic files in CIF format for the structure determination of [*fac*-$Ru(OCOCF_3)_2(CO)_3(H_2O)$], [*fac*-$Ru(CO)_3(H_2O)_3][BF_4]_2$, $[Ru_2(C_2H_5)_2(CO)_4(H_2O)_4][CF_3SO_3]_2$, and $[Ru_4(C(O)C_2H_5)_4(OH)_2(CF_3SO_3)_2(CO)_8]$. This material is available free of charge via the Internet at http://pubs.acs.org.

IC981429I